

Structure and Bonding of (μ -Dicarbido)hexa-*tert*-butoxyditungsten, (*t*-BuO)₃W \equiv C—C \equiv W(O-*t*-Bu)₃

Kenneth G. Caulton,* Roger H. Cayton, Malcolm H. Chisholm,* John C. Huffman,
Emil B. Lobkovsky, and Ziling Xue

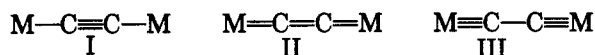
Department of Chemistry and Molecular Structure Center, Indiana University, Bloomington, Indiana 47405

Received June 14, 1991

The molecular structure of (*t*-BuO)₃W \equiv C—C \equiv W(O-*t*-Bu)₃ (1) has been determined by single-crystal X-ray crystallography at -171 °C. The compound crystallizes with two toluene molecules in the triclinic system, space group $P\bar{1}$, with $a = 10.926$ (7) Å, $b = 15.706$ (12) Å, $c = 9.674$ (6) Å, $\alpha = 90.99$ (5)°, $\beta = 90.27$ (4)°, $\gamma = 82.59$ (5)°, $V = 1646.1$ Å³, and $Z = 1$. The two W(O-*t*-Bu)₃ groups are arranged in the staggered conformation. The C—C bond length of 1.34 (3) Å in the bridge W \equiv C—C \equiv W moiety parallels that in H—C \equiv C—C \equiv H (1.384 (2) Å). The W \equiv C bond length of 1.819 (16) Å is somewhat longer than that in most tungsten alkylidyne complexes. The UV-visible spectrum of 1 in hexane shows five absorptions at 430 (2490 M⁻¹ cm⁻¹), 354 (7590 M⁻¹ cm⁻¹), 294 (11 300 M⁻¹ cm⁻¹), 254 (27 800 M⁻¹ cm⁻¹), and 246 (26 800 M⁻¹ cm⁻¹) nm. Cyclic voltammetry measurements in CH₂Cl₂ with *n*-Bu₄NPF₆ (*n*-Bu = CH₃CH₂CH₂CH₃) as the supporting electrolyte reveal two irreversible oxidations at 0.362 and 0.816 V vs a saturated calomel electrode (SCE) reference. A MO calculation employing the Fenske-Hall method on the model compound (HO)₃WC₂W(OH)₃ indicates that the C₂ ligand is both a strong π -donor and strong π -acceptor, which leads to an approach of the limiting valence bond description W \equiv C—C \equiv W for the central moiety. A comparison is made with the established chemistry of linear bridged dinitrogen complexes.

Introduction

Complexes that contain a C₂ bridging unit between two metal atoms have been of interest in terms of their structure and bonding. Three limiting valence bond descriptions of a central linear M—C—C—M moiety can be drawn as shown in I–III.



Cp(CO)_{*n*}M—C \equiv C—M(CO)_{*n*}Cp (Cp = η^5 -cyclopentadienyl; M = W, $n = 3$;^{1a} M = Ru, $n = 2$;^{1b}), (OC)₅Re—C \equiv C—Re(CO)₅,² X(PR₃)₂M—C \equiv C—M(PR₃)₂X (M = Pd, Pt; R = Me, Et, *n*-Bu; X = Cl, I),³ and (η^5 -C₅Me₅)₂Sc—C \equiv C—Sc(η^5 -C₅Me₅)₂^{4a} with an ethynediyl bridge have been synthesized with molecular structures consistent with description I. Other complexes depicted by I have also been reported.^{4b-d}

Recently (*t*-Bu₃SiO)₃Ta(μ -C₂)Ta(OSi-*t*-Bu₃)₃ was reported.⁵ The bond distances and electronic structure are consistent with the description shown in II involving a central C₂⁴⁻ ligand. The compound (*t*-BuO)₃W \equiv C—C \equiv W(O-*t*-Bu)₃ (1) was first synthesized through scission of 3,5-octadiyne by W₂(O-*t*-Bu)₆.⁶ 1 is preferentially formed

(1) (a) Chen, M.-C.; Tsai, Y.-J.; Chen, C.-T.; Lin, Y.-C.; Tseng, T.-W.; Lee, G.-H.; Wang, Y. *Organometallics* 1991, 10, 378. Ustynyuk, N. A.; Vinogradova, V. N.; Kravtsov, D. N.; Oprunenko, Y. F.; Piven, V. A. *Metalloorg. Khim.* 1988, 1, 884; *Chem. Abstr.* 1989, 111, 233074C. (b) Koutsantonis, G. A.; Selegue, J. P. *J. Am. Chem. Soc.* 1991, 113, 2316.

(2) (a) Heidrich, J.; Steimann, M.; Appel, M.; Beck, W.; Phillips, J. R.; Troglor, W. C. *Organometallics* 1990, 9, 1296. (b) Appel, M.; Heidrich, J.; Beck, W. *Chem. Ber.* 1987, 120, 1087. (c) Beck, W.; Niemer, B.; Breimair, J.; Heidrich, J. *J. Organomet. Chem.* 1989, 372, 79.

(3) Ogawa, H.; Onitsuka, K.; Joh, T.; Takahashi, S.; Yamamoto, Y.; Yamazaki, H. *Organometallics* 1988, 7, 2257.

(4) (a) St. Clair, M.; Schaefer, W. P.; Bercaw, J. E. *Organometallics* 1991, 10, 525. (b) Cr: Ustynyuk, N. A.; Vinogradova, V. N.; Kravtsov, D. N. *Metalloorg. Khim.* 1988, 1, 85–88; *Chem. Abstr.* 1989, 110, 231804W. (c) V: Kreisel, G.; Scholz, P.; Seidel, W. Z. *Anorg. Allg. Chem.* 1980, 460, 51. (d) Au: Nast, R.; Schneller, P.; Hengefeld, A. *J. Organomet. Chem.* 1981, 214, 273. Cross, R. J.; Davidson, M. F.; McLennan, A. J. *J. Organomet. Chem.* 1984, 265, C37.

(5) Neithamer, D. R.; LaPointe, R. E.; Wheeler, R. A.; Richeson, D. S.; Van Duyne, G. D.; Wolozanski, P. T. *J. Am. Chem. Soc.* 1989, 111, 9056.

(6) Listemann, M. L.; Schrock, R. R. *Organometallics* 1985, 4, 74.

Table I. Summary of Crystal Data

empirical formula	(Me ₂ CO) ₃ W \equiv C—C \equiv W(OCMe ₃) ₃ 2C ₆ H ₅ CH ₃
color of cryst	orange/red
cryst dimens, mm	0.25 × 0.20 × 0.10
space group	$P\bar{1}$
temp, °C	-171
cell dimens	
<i>a</i> , Å	10.926 (7)
<i>b</i> , Å	15.706 (12)
<i>c</i> , Å	9.674 (6)
α , deg	90.99 (5)
β , deg	90.27 (4)
γ , deg	82.59 (5)
<i>Z</i> (molecules/cell)	1
<i>V</i> , Å ³	1646.09
calcd density, g/cm ³	1.024
wavelength, Å	0.71069
mol wt	1014.68
linear abs coeff, cm ⁻¹	35.917
2θ range, deg	6–45
total no. of rflns collected	2900
no. of unique intensities	2149
no. with $F_o > 0.0$	2076
no. with $F_o > 2.33(F)$	1993
<i>R</i> (<i>F</i>)	0.0553
<i>R</i> _w (<i>F</i>)	0.0560
goodness of fit for the last cycle	1.567
max Δ/σ for last cycle	0.30

presumably due to its low reactivity toward metathesis. As a minor product, 1 was later synthesized from the reaction of *trans*-Pt(C \equiv CH)₂(PMe₂Ph)₂ and W₂(O-*t*-Bu)₆.⁷ The bonding description of III was formulated on the basis of the analogy with tungsten(6+) alkylidynes of formula (RO)₃W \equiv CR and on the observed value of ¹*J*_{18C-18C} for the central C₂ moiety. Here we report the molecular structure, UV-visible spectrum, and cyclic voltammogram of compound 1, together with a discussion of the bonding in the central W—C—C—W moiety based on a calculation employing the Fenske-Hall method.

(7) Blau, R. J.; Chisholm, M. H.; Folting, K.; Wang, R. J. *J. Am. Chem. Soc.* 1987, 109, 4552.

Table II. Fractional Coordinates and Isotropic Thermal Parameters for the $(\text{Me}_3\text{CO})_3\text{W}=\text{C}-\text{C}=\text{W}(\text{OCMe}_3)_3$ Molecule

atom	10^4x	10^4y	10^4z	$10B_{\text{iso}}, \text{\AA}^2$
W(1)	1680 (1)	931.2 (5)	45 (1)	14
C(2)	1161 (9)	1928 (6)	1058 (11)	18
O(3)	3026 (9)	259 (6)	888 (10)	15
O(4)	2056 (9)	1209 (7)	-1773 (10)	18
C(5)	126 (14)	2456 (11)	1730 (17)	23
C(6)	-663 (16)	2919 (10)	635 (17)	24
C(7)	662 (16)	3065 (11)	2681 (17)	26
C(8)	-593 (15)	1836 (11)	2510 (16)	23
C(9)	3331 (14)	-519 (10)	1615 (15)	18
C(10)	4705 (16)	-652 (11)	1781 (18)	26
C(11)	2904 (16)	-1228 (12)	751 (17)	27
C(12)	2666 (16)	-449 (12)	2952 (17)	27
C(13)	1536 (15)	1120 (11)	-1352 (15)	22
C(14)	1386 (16)	223 (11)	-3473 (17)	25
C(15)	2447 (17)	1466 (12)	-4143 (17)	30
C(16)	284 (16)	1744 (12)	-3174 (17)	28
C(17)	452 (15)	251 (10)	0 (15)	19
C(S1)	6911 (23)	6332 (16)	5809 (27)	49 (5)
C(S2)	6477 (22)	5530 (16)	4348 (26)	47 (6)
C(S3)	6219 (29)	6525 (21)	5052 (32)	67 (6)
C(S4)	7194 (27)	5336 (19)	5149 (31)	62 (6)

Table III. Bond Distances (\AA) for the $(\text{Me}_3\text{CO})_3\text{W}=\text{C}-\text{C}=\text{W}(\text{OCMe}_3)_3$ Molecule

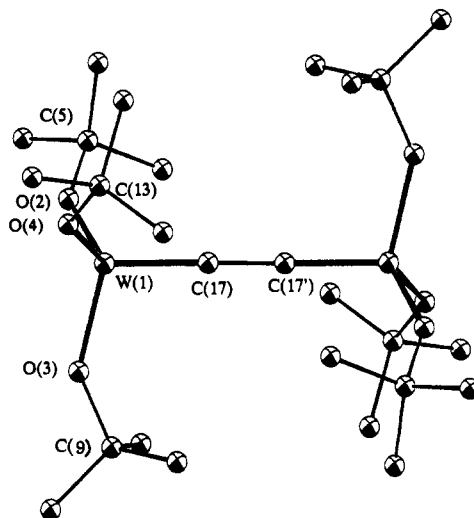
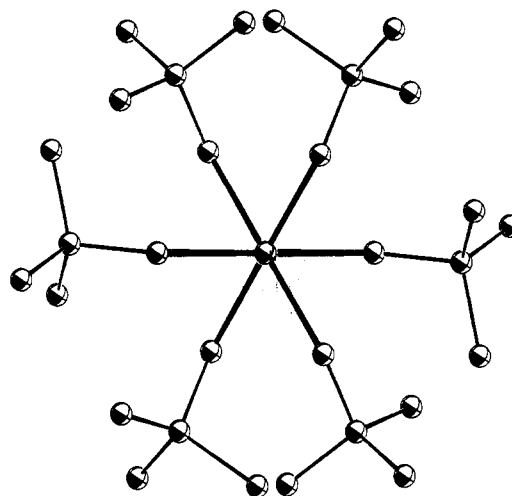
W(1)-O(2)	1.859 (10)	C(5)-C(8)	1.537 (22)
W(1)-O(3)	1.887 (10)	C(9)-C(10)	1.497 (23)
W(1)-O(4)	1.879 (10)	C(9)-C(11)	1.502 (23)
W(1)-C(17)	1.819 (16)	C(9)-C(12)	1.482 (22)
O(2)-C(5)	1.461 (19)	C(13)-C(14)	1.467 (24)
O(3)-C(9)	1.422 (18)	C(13)-C(15)	1.540 (22)
O(4)-C(13)	1.459 (18)	C(13)-C(16)	1.577 (23)
C(5)-C(6)	1.501 (24)	C(17)-C(17')	1.34 (3)
C(5)-C(7)	1.488 (24)		

Table IV. Bond Angles (deg) for the $(\text{Me}_3\text{CO})_3\text{W}=\text{C}-\text{C}=\text{W}(\text{OCMe}_3)_3$ Molecule

O(2)-W(1)-O(3)	112.1 (4)	C(7)-C(5)-C(8)	112.2 (14)
O(2)-W(1)-O(4)	109.9 (5)	C(3)-C(9)-C(10)	107.0 (12)
O(2)-W(1)-C(17)	109.3 (6)	C(3)-C(9)-C(11)	107.5 (12)
O(3)-W(1)-O(4)	111.4 (4)	C(3)-C(9)-C(12)	108.8 (12)
O(3)-W(1)-C(17)	104.9 (6)	C(10)-C(9)-C(11)	110.8 (13)
O(4)-W(1)-C(17)	109.1 (6)	C(10)-C(9)-C(12)	113.1 (13)
W(1)-O(2)-C(5)	146.4 (9)	C(11)-C(9)-C(12)	109.4 (14)
W(1)-O(3)-C(9)	141.6 (9)	O(4)-C(13)-C(14)	111.2 (13)
W(1)-O(4)-C(13)	137.4 (9)	O(4)-C(13)-C(15)	105.4 (13)
O(2)-C(5)-C(6)	108.5 (13)	O(4)-C(13)-C(16)	106.0 (12)
O(2)-C(5)-C(7)	106.9 (13)	C(14)-C(13)-C(15)	112.0 (14)
O(2)-C(5)-C(8)	106.4 (13)	C(14)-C(13)-C(16)	113.4 (14)
O(3)-C(9)-C(10)	111.6 (14)	C(15)-C(13)-C(16)	108.4 (14)
O(3)-C(9)-C(11)	110.9 (13)	W(1)-C(17)-C(17')	178.6 (17)

Results and Discussion

Structure of $(t\text{-BuO})_3\text{W}=\text{C}-\text{C}=\text{W}(\text{O}-t\text{-Bu})_3$ (1). Crystals of 1 that were used in the X-ray crystallographic analysis were obtained from toluene solution. Crystallographic data, atom positions, selected bond lengths, and bond angles are presented in Tables I-IV. ORTEP views of 1 in the crystal form are shown in Figures 1 and 2. The molecule is oriented around the crystallographic center of symmetry. The tungsten atoms and alkylidyne atoms are basically collinear, as shown in Figure 1. The two $\text{W}(\text{O}-t\text{-Bu})_3$ moieties are arranged in a staggered conformation, which has similarly been observed in $(t\text{-Bu}_3\text{SiO})_3\text{Ta}=\text{C}=\text{C}=\text{Ta}(\text{OSi}-t\text{-Bu}_3)_3$,⁵ $\text{I}(\text{Me}_3\text{P})_2\text{Pt}-\text{C}\equiv\text{C}-\text{Pt}(\text{PMe}_3)_2\text{I}$,³ and *trans*- $\text{Cp}(\text{CO})_2\text{Ru}-\text{C}\equiv\text{C}-\text{Ru}(\text{CO})_2\text{Cp}$.^{1b} In contrast, the structure of $(\text{OC})_5\text{ReC}\equiv\text{CRe}(\text{CO})_5$ shows an eclipsed conformation.² The four groups around each W atom in 1 present a pseudotetrahedral geometry with bond angles among each of the two groups ranging from 104.9 (6) to 112.1 (4)°. The geometry is similar to the pseudotetra-

**Figure 1.** ORTEP drawing of $(t\text{-BuO})_3\text{W}=\text{C}-\text{C}=\text{W}(\text{O}-t\text{-Bu})_3$ (1), showing the atom number scheme.**Figure 2.** View of 1 down the WCCW axis, showing the staggered arrangement of the *t*-BuO ligands.

hedral arrangement observed in the structure of $(\text{Me}_3\text{CCH}_2)_3\text{W}=\text{CSiMe}_3$.⁸

Comments on the C_2 Bond Length in 1. Prior to a discussion of the bonding, it is good to appreciate the structural parameters observed for the linear WCCW moiety. In addition to our present structural characterization of the title compound, Gilbert and Rogers⁹ have independently determined the structure of 1, and in their crystals there was not the problem of partial occupancy of solvent molecules. The essential features of the molecular structure were the same, and they determined $\text{W}-\text{C} = 1.79$ (1) \AA and $\text{C}-\text{C} = 1.38$ (2) \AA . These distances are equivalent to those in the present structure, at least within the criteria of 3σ . The $\text{W}-\text{C}$ distance of 1.79 (1) \AA , however, appears within the range of typical $\text{W}-\text{C}$ triple-bond distances in $\text{X}_3\text{W}=\text{CR}$ compounds, 1.76 (1) \AA (av).¹⁰ Suffice it to say that the $\text{W}-\text{C}$ distance of either 1.79 (1) or 1.82 (2) \AA is close to the distance expected for a $\text{W}-\text{C}$

(8) Caulton, K. G.; Chisholm, M. H.; Streib, W.; Xue, Z. *J. Am. Chem. Soc.* 1991, 113, 6082.

(9) Gilbert, T. M.; Rogers, R. D. Personal communication.

(10) $\text{W}=\text{C}$ bond lengths are normally in the range of 1.74-1.80 \AA . See: Nugent, W. A.; Mayer, J. M. *Metal-Ligand Multiple Bonds*; Wiley: New York, 1988. Schubert, U. In *Carbyne Complexes*; Fischer, H., Hoffmann, P., Kreissl, F. R., Schrock, R. R., Schubert, U., Weiss, K., Eds.; VCH: New York, 1988.

Table V. Comparisons of Carbon-Carbon Bond Lengths and Coupling Constants for Compounds with Multiple Bonds to Carbon

compd	C-C bond length, Å	C-C coupling const, Hz
H-C≡C-C≡C-H	1.384 (2) (C ₂ -C ₃) ^{a,c} 1.218 (2) (C ₁ -C ₂)	154.9 (2) (C ₂ -C ₃) ^d 194.1 (1) (C ₁ -C ₂)
H ₂ C=C=C=CH ₂	1.284 (6) (C ₂ -C ₃) ^{b,e} 1.309 (3) (C ₁ -C ₂)	156.6 (C ₂ -C ₃ , calcd) ^f 120.7 (C ₁ -C ₂ , calcd)
H-C≡C-H	1.207 ^b 1.212 (2) ^a	171.5 ^f
(Bu- <i>t</i> -O) ₃ W=C-C≡ W(O- <i>t</i> -Bu) ₃	1.34 (4) ^g 1.38 (2) ^h	44.5 ⁱ
(silox) ₃ Ta=C=C= Ta(silox) ₃	1.37 (4) ^j	
Cp(CO) ₃ W-C=C- W(CO) ₃ Cp	1.18 (3) ^k	
(OC) ₃ Re-C≡C-Re(CO) ₃	1.195 (33) ^l	

^a Reference 11. ^b Stoicheff, B. P. *Tetrahedron* **1962**, *17*, 135. ^c Tanimoto, M.; Kuchitsu, K.; Morino, Y. *Bull. Chem. Soc. Jpn.* **1971**, *44*, 386. ^d Kamienska-Trela, K. *Org. Magn. Reson.* **1980**, *14*, 398. ^e Stoicheff, B. P. *Can. J. Phys.* **1957**, *35*, 837. ^f Reference 12. ^g This work. ^h Reference 9. ⁱ Blau, R. J.; Chisholm, M. H.; Folting, K.; Wang, R. J. *J. Am. Chem. Soc.* **1987**, *109*, 4552. ^j Silox = *t*-Bu₃SiO⁻; Neithamer, D. R.; LaPointe, R. E.; Wheeler, R. A.; Richeson, D. S.; Van Duynne, G. D.; Wolczanski, P. T. *J. Am. Chem. Soc.* **1989**, *111*, 9056. ^k Reference 1a. ^l Reference 2.

triple bond, albeit a little on the long side. A C-C distance of 1.34 (4) or 1.38 (2) Å is more difficult to place because (i) the esd's provide considerable latitude and (ii) C-C single- and double-bond distances are commonly considered to be 1.54 and 1.34 Å, as seen in diamond and ethylene, respectively.¹¹ The latter neglects to consider the hybridization at carbon, and this makes an important contribution.

In Table V we present some comparative data for compounds containing multiple bonds to carbon in linear arrangements. The central C-C distance in 1,3-butadiyne is seen to be essentially the same as that in **1** and provides the most pertinent comparison for the VB description III. The central C-C distance in butatriene (1.284 (6) Å) is notably shorter, and the C≡C distances in [CpW(CO)₃]₂(μ-C₂) and [(CO)₅Re]₂(μ-C₂) are only slightly longer than those in ethyne and 1,3-butadiyne.

C-C carbon-13 coupling constants provide a good measure of C 2s character and often are helpful in determining the hybridization at carbon. Compare, for example, ¹J_{13C-13C} = 171, 67, and 36 Hz in ethyne, ethene, and ethane¹² and 154.9 (2) Hz (C₂-C₃) in HC≡C-C≡CH (Table V). The exceptionally low value of ¹J_{13C-13C} = 44 Hz in **1** is almost certainly a reflection of the greater affinity of C 2s bonding to tungsten (relative to its other neighbor C) and parallels the extremely small value of ¹J_{13C-1H} in (*t*-BuO)₃W≡CH¹³ (150 Hz), compared to that of HC≡CH (¹J_{13C-1H} = 250 Hz).

Bonding Considerations. The bonding in this dinuclear compound can readily be anticipated from the calculations of Wolczanski and co-workers⁵ for [(silox)₃Ta]₂(μ-C₂) by the addition of two electrons. However, it is instructive to consider the bonding in **1** by a fragment approach wherein two d³-W(OH)₃ units are added to the C₂ molecule along the C-C axis such that the molecule has

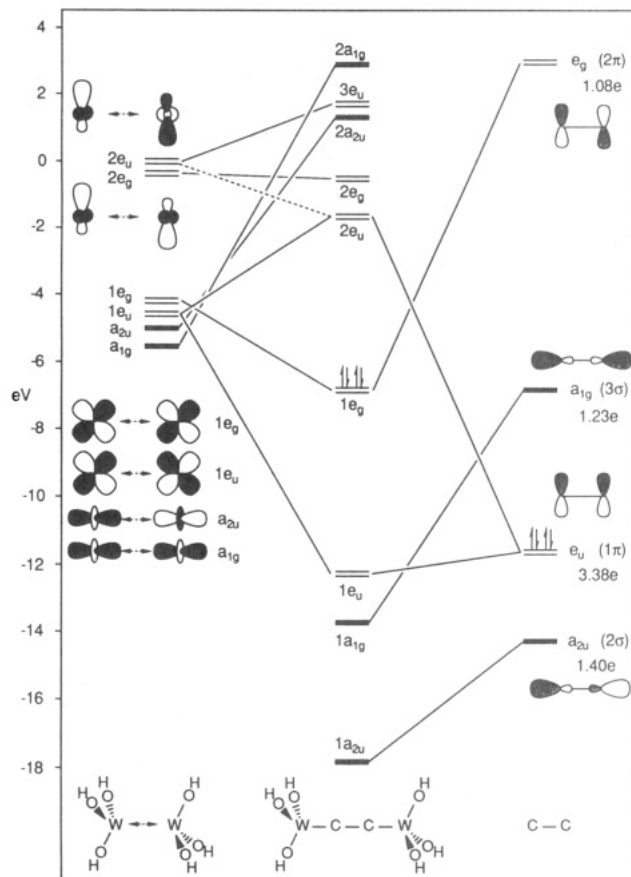


Figure 3. Frontier orbital diagram of (HO)₃WCCW(OH)₃ depicting the interaction of two (HO)₃W fragments with a C₂ moiety. The double-headed arrows between the (HO)₃W fragments indicate a 5-Å separation and no direct M-M bond. The HOMO is indicated by single-headed arrows. The Mulliken populations of the C₂ orbitals are beneath them. The dotted line corresponds to a minor contribution to the resulting character of the molecular orbital. In D_{3d} symmetry the z axis is coincident with the C₃ axis that contains the linear WCCW unit.

D_{3d} symmetry. In this way we can address the question of M-C and C-C bond order and relate the results of the calculations to the limiting valence bond (VB) descriptions, I-III, and the bonding in the C₂ diatomic molecule. We have employed the Fenske-Hall calculational method and substituted hydrogen atoms for *t*-Bu groups. The other parameters for the central O₃WC₂WO₃ moiety were taken from the structure of **1** and were idealized to D_{3d} symmetry.¹⁴

On the left-hand side of Figure 3 we show the frontier orbitals of two (HO)₃W fragments separated by ca. 5 Å. This leads to the sets of σ/σ*, π/π*, and δ/δ* orbitals shown. The δ-orbitals depicted in Figure 3 are the result of mixing with W 6p atomic orbitals in the manner shown in IV. At a distance of 5 Å two d³-ML₃ fragments would not yield a M-M triple bond of valence configuration σ²π⁴ as in (RO)₃W≡W(OR)₃ with M-M = 2.3 Å.

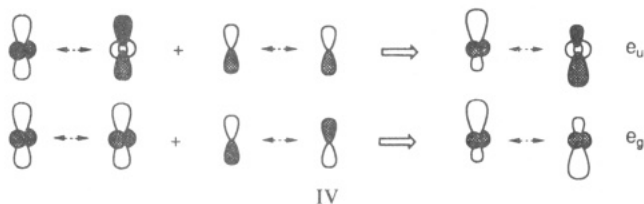
On the right-hand side of Figure 3, we show the frontier orbitals of the diatomic molecule C₂ at a C-C distance of 1.34 Å. There is a distinct resemblance in the ordering of

(14) The O₃WCCWO₃ core of **1** was idealized to D_{3d} symmetry using C-W-O angles of 106°. In this geometry the orbitals of the e_g and e_g sets do not lie on (or perpendicular to) any of the C-W-O planes such that they are difficult to represent pictorially. Therefore, two of the six C-W-O angles were reduced to 104° to lower the absolute symmetry of the model compound to C_{2h}. This slight geometrical change does not alter the electronic structure but forces the "e" sets to lie on or 90° to the C-W-O planes, making them easier to represent. D_{3d} symmetry labels were maintained for simplicity.

(11) Kuchitsu, K. In *Molecular Structure and Properties*; Buckingham, A. D., Allen, G., Eds.; University Park Press: Baltimore, MD, 1972; MTP International Review of Science, Physical Chemistry, Series One, Vol. 2, p 203.

(12) Stothers, J. B. *Carbon-13 NMR Spectroscopy*; Academic Press: New York, 1973; Table 9.3, p 327.

(13) Chisholm, M. H.; Folting, K.; Hoffman, D. M.; Huffman, J. C. *J. Am. Chem. Soc.* **1984**, *106*, 6794.



the frontier orbitals to that in C_2 with a distance of 1.24 Å.¹⁵ The HOMO is the C-C π bond, and the LUMO is a C-C σ -bonding orbital having mostly p_z - p_z character. There are two other σ orbitals. The one which is shown, the SHOMO, is C-C antibonding, being principally C 2s-C 2s but with some mixing of C 2p_z. The occupied C-C σ -bonding MO that is not shown in Figure 3 is formed from C 2s-C 2s, again with C 2p mixing.

When the three fragments are brought together to form $(HO)_3WCCW(OH)_3$, several interesting interactions occur.

(1) The in- and out-of-phase σ orbitals from the two $W(OH)_3$ fragments ($1a_{2g}$, $1a_{2u}$) interact with the C_2 3 σ and 2 σ orbitals, respectively. The C_2 2 σ orbital, which is C-C antibonding, donates electron density (0.6 e) to the tungsten atoms, whereas the metal donates electron density (1.23 e) to the originally vacant C_2 3 σ orbital. Both of these interactions might be expected to lead to enhanced C-C σ bonding in **1** relative to that in the C_2 fragment with $d = 1.34$ Å. However, the net C-C σ overlap population change is essentially negligible and as such presumably reflects the formal lone-pair character of the 2 σ and 3 σ orbitals of the C_2 fragment.

(2) The π bonding can be broken down into C_2 acting as a π donor and a π acceptor, both of which will lead to a decrease in C-C π -bond order. The filled C_2 π orbital, $1\pi_u$, interacts with the $1e_u$ W d_π orbitals of the two $(HO)_3W$ fragments to donate 0.31 e per π bond. In this way the C_2 moiety behaves similarly to an oxo or linear imido ligand. In addition, the δ -type orbitals of e_u symmetry are also involved in this interaction, as they mix with the lower energy metal-based e_u set. The LUMO is the $2e_u$ orbital and is comprised of 92% $[(HO)_3W]_2$ character and only 8% C_2 ; i.e., it is metal-centered.

The second type of π interaction involves the unoccupied C_2 π^* orbitals and the metal-based d_π orbitals of e_g symmetry. This interaction generates the HOMO that is 74% metal-based and 26% C_2 in character. The π^* of C_2 formally accepts 0.54 e per π bond. The combined effects of C_2 π donation and C_2 π^* acceptance leads to a decrease of the π overlap population in the C_2 fragment by 75% upon interaction. Alternatively expressed, 25% of the C-C π bonding remains in **1**. Thus, the calculations indicate that the limiting VB description of **III** is approached but not reached.

It is worthy of note that the later transition elements, or complexes with all filled d_π electrons, will not serve to reduce the C-C bond order to the same extent: (1) The early transition metals are more electropositive, and in the absence of additional π -acceptor ligands, M d_π to C_2 π^* donation will be favored. (2) If all the metal d_π orbitals are filled, as is the case for $(CO)_5ReCCR(CO)_5$ ² and $(X)L_2PtC_2PtL_2(X)$,³ then no net C-C π donation is possible.

Physicochemical Properties of $(t-BuO)_3W\equiv C-C\equiv W(O-t-Bu)_3$ (1**).** Two irreversible oxidation processes have been observed for **1** with $E_p^1 = 0.362$ V and $E_p^2 = 0.816$ V (200 mV/s scan) vs the SCE reference electrode or -0.354 and 0.100 V vs ferrocene in dichloromethane

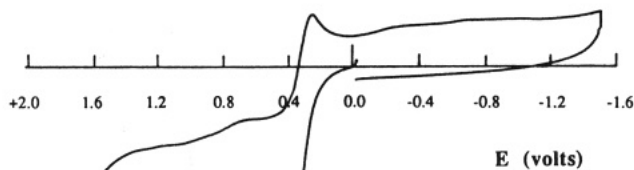


Figure 4. Cyclic voltammogram of **1** in CH_2Cl_2 . The supporting electrolyte is 0.1 M $(n-Bu)_4NPF_6$, and the scan rate is 200 mV/s.

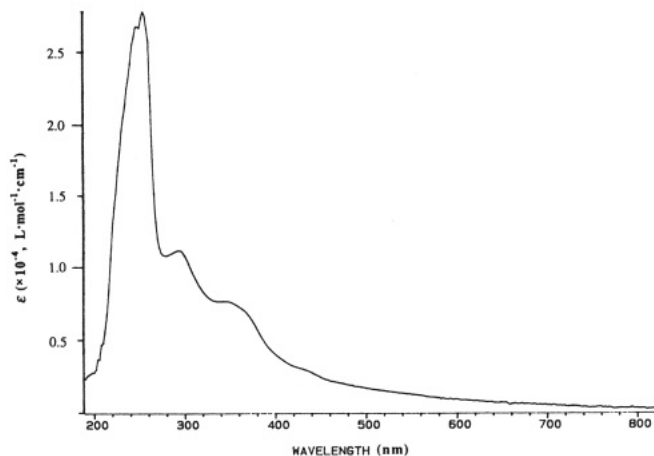


Figure 5. Electronic absorption spectrum of a 0.129 mM solution of **1** in hexane.

solution (Figure 4). Both oxidation waves were shown to be one-electron processes by comparing the current flow to that of an equimolar solution of ferrocene under the same conditions. The magnitude of the second oxidation wave is quite scan rate dependent. At 1000 mV/s the current of the second wave corresponds to a one-electron oxidation, but at rates <100 mV/s the wave virtually disappears. This is consistent with the production of the relatively unstable monocation $(t-BuO)_3W\equiv C-C\equiv W(O-t-Bu)_3^+$ by the first oxidation wave, which then decomposes before undergoing a second oxidation at slow scan rates. The difference in potential between the two one-electron oxidations is 454 mV, indicating that the unpaired electron in the monocation is delocalized over the $W\equiv C-C\equiv W$ core and is not mixed valence. The very unstable dication of **1** would be isoelectronic with the previously isolated TaCCTa silox complex.⁵ No reduction processes were observed to -1.6 V in CH_2Cl_2 solution.

It is interesting to note that since the HOMO of **1** was calculated to be W-C π bonding and C-C π antibonding (Figure 3), whereas the LUMO is W-C π antibonding and C-C π bonding, both oxidation and reduction should serve to weaken the W-C bond and strengthen the C-C bond. In other words, the neutral species **1** contains the ideal electron count to minimize the C-C bond order and approach the limiting VB description **III**.

The electronic absorption spectrum of **1** shows the presence of several resolved electronic transitions (Figure 5). The lowest energy absorption falls into the visible region at 430 nm with relatively weak intensity (2490 M⁻¹ cm⁻¹), giving rise to the red color of **1** in solution. In concentrated solution (1 mmol), the presence of the visible absorption clearly emerges. The UV absorptions are more intense absorptions at 354 (7590 M⁻¹ cm⁻¹), 294 (11300 M⁻¹

(15) See, for example: DeKock, R. L.; Gray, H. B. *Chemical Structure and Bonding*; Benjamin/Cummings: Menlo Park, CA, 1980; p 231.

cm^{-1}), 254 ($27800 \text{ M}^{-1} \text{ cm}^{-1}$), and 246 ($26800 \text{ M}^{-1} \text{ cm}^{-1}$) nm. It is quite reasonable to assign the lower energy absorption at 430 nm to the singlet HOMO \rightarrow LUMO transition which is orbitally allowed in D_{3d} symmetry.

Concluding Remarks. This work provides the structural characterization of a compound containing a central unit for which the VB description $\text{M}\equiv\text{C}-\text{C}\equiv\text{M}$ (III) is approached. This complements earlier work wherein the other two VB descriptions I and II are appropriate.

The fragment molecular orbital approach, wherein the molecule is constructed as a sandwich containing a central neutral C_2 molecule bracketed by two L_nM fragments, is useful in terms of providing a general understanding of $\mu\text{-C}_2$ -containing compounds. The situation lends itself to an appreciation of the significance of electron count and orbital energetics. For a given oxidation state the effect of increasing electronegativity across the transition series will lead to a lowering of the metal d_π orbital energies from left to right. This leads to the now well-accepted fact that, for example, Zr^{2+} , a d^2 ion, is a much more powerful reducing agent than Pd^{2+} , a d^8 ion. From this factor alone we would expect that the early and middle transition elements would show greater $\text{M } d_\pi\text{-to-} \text{C}_2 \pi^*$ back-bonding than the later transition elements. When there are also vacant metal d_π orbitals to accept electron density from the filled $\text{C}_2 \pi$ orbitals, this will lead to a further reduction of C-C bond order and an enhancement of M-C multiple bonding. The optimum electron count for the VB description III is seen for a $d^3\text{-X}_3\text{W}$ fragment. In the absence of vacant d_π orbitals to receive electron density, the C_2 fragment can only be reduced in the ionic sense, as in binary and ternary metal carbides, where there is formally a C_2^{6-} unit with a C-C single bond.¹⁶

Finally, it is worth noting a parallel with the chemistry of linear bridged dinitrogen complexes. The dinitrogen molecule is isoelectronic with C_2^{2-} and has an element-element triple bond and two σ -type lone pairs. In $[(\text{H}_3\text{N})_5\text{Ru}]_2(\mu\text{-N}_2)^{4+}$ two $d^6\text{-Ru}^{\text{II}}$ centers sandwich the N_2 ligand. The N-N distance of 1.124 (15) Å is only marginally longer than that found in the N_2 molecule, 1.097 (2) Å.¹⁷ The Ru d_π orbitals are filled, and so only back-bonding to the $\text{N}_2 \pi^*$ orbitals is possible and this is evidently only modest. This can be contrasted with the stereochemically correspondent $d^2\text{-Ta}^{3+}$ complexes of general formula $[\text{TaCl}_3(\text{L})_2]_2(\mu\text{-N}_2)$ prepared by Schrock and co-workers.¹⁸ Here there are vacant metal d_π orbitals as well as filled d_π orbitals such that the N-N bond is reduced by both $\text{N}_2 \pi^*$ acceptance and by $\text{N}_2 \pi$ donation. The N-N distance of 1.282 (6) Å in $[\text{TaCl}_3(\text{P}(\text{CH}_2\text{Ph})_3)(\text{THF})_2(\mu\text{-N}_2)]_2 \cdot 0.7\text{CH}_2\text{Cl}_2$ is approaching that of a N-N single bond.¹⁹ Similarly long N-N distances have more recently been reported for $[\text{Cp}^*\text{WMe}_2(\text{OC}_6\text{F}_5)_2]_2(\mu\text{-N}_2)$,²⁰ $[\text{Cp}^*\text{WMe}_2(\text{S-2,4,6-C}_6\text{H}_2\text{Me}_3)_2]_2(\mu\text{-N}_2)$,²⁰ and $[\text{Cp}^*\text{MoMe}_3]_2(\mu\text{-N}_2)$,²¹ all of which contain a central N_2 unit sandwiched between two $d^2\text{-ML}_n$ fragments with vacant metal d_π orbitals. In contrast, the well-known linear bridged N_2 complex of Bercaw et al.²² $[\text{Cp}_2^*\text{Zr}(\eta^1\text{-N}_2)]_2$

has a N-N distance of 1.182 (5) Å. The N_2 moiety is sandwiched between two $d^2\text{-ML}_n$ centers that formally lack vacant d_π orbitals. The valence electron count at each zirconium is 18 as a result of coordination to two $\eta^5\text{-Cp}^*$ ligands and formation of two σ bonds, one to each of the η^1 and $\mu\text{-N}_2$ ligands.

Experimental Section

All manipulations were carried out under a N_2 atmosphere. $(t\text{-BuO})_3\text{W}\equiv\text{C}-\text{C}\equiv\text{W}(\text{O-}t\text{-Bu})_3$ (1) was synthesized according to the literature method.⁶ Recrystallization from hot toluene solution gave red crystals. The toluene had been distilled from a Na/benzophenone solution under a N_2 atmosphere.

X-ray Crystal Structure Determination. General procedures and listings of programs have been previously reported.²³

A crystal of suitable size was mounted using silicone grease and was transferred to a goniostat, where it was cooled to -171°C for characterization and data collection. A systematic search of a limited hemisphere of reciprocal space revealed no symmetry or systematic absences. An initial choice of space group $P\bar{1}$ was confirmed by the successful solution of the structure. No correction was made for absorption.

The structure was solved by a combination of Patterson methods and Fourier techniques. The W atom positions were obtained from the Patterson map, and the remainder of the non-hydrogen atoms were found in subsequent iterations of least-squares refinement and difference Fourier calculations. Hydrogen atoms were included in fixed calculated positions with thermal parameters fixed at 1 \AA^2 plus the thermal parameter of the atom to which it was bonded.

The final cycles of least-squares refinement of the non-hydrogen atoms were varied with anisotropic thermal parameters to $R(F) = 0.055$. The final difference map was reasonably clean. There were tungsten residuals of $1.0\text{--}1.1 \text{ e/\AA}^3$.

The density of the crystal, 1.02 g/cm^3 , is extremely low. There is a huge void in the center of the cell. The "tunnel", about 9 Å in diameter, goes along the z axis, containing disordered solvent molecules. The four atoms C(S1)–C(S4), representing the solvent molecule, are nearly coplanar. Therefore, we assume that the solvent is toluene or benzene. Linked "tunnels" form layers which alternate with the tungsten compound layers along the y direction.

Electrochemical Measurements. CH_2Cl_2 was distilled from CaH_2 under N_2 . Tetra- n -butylammonium hexafluorophosphate, $(n\text{-Bu})_4\text{NPF}_6$ (Aldrich), was used under an Ar atmosphere.

Cyclic voltammetry measurements were carried out with the use of a IBM EC/225 voltammetric analyzer and a EG&G PAR (Model 175) universal programmer. In a drybox 387.4 mg of $(n\text{-Bu})_4\text{NPF}_6$ and 9.1 mg of 1 were dissolved in 10.0 mL of CH_2Cl_2 to make 0.1 M $(n\text{-Bu})_4\text{NPF}_6$ and 1.1 mM 1 under a He atmosphere. The solution was then placed in a preassembled electrochemical cell. A saturated calomel electrode (SCE) was used as a reference. A platinum-disk electrode and carbon electrode were used to measure voltage and current. The cyclic voltammograms were recorded at several scan rates from 200 to 500 mV/s.

UV-Visible Spectroscopy. Hexane was distilled from K/benzophenone under nitrogen. A 0.129 mM solution was prepared under N_2 . The electronic absorption spectrum of the solution was recorded from 700 to 200 nm.

Computational Details. The atomic positions for the model complex $(\text{HO})_3\text{WCCW}(\text{OH})_3$ were taken from the crystal structure of 1 and idealized as outlined in ref 14. An O-H distance of 0.96 Å was used, and the W-O-H angles were constrained to be linear. The Fenske-Hall MO method²⁴ was employed for the calculations. All atomic wave functions were generated by using the method of Bursten, Jensen, and Fenske.²⁵ Contracted double- ζ representations were used for the W 5d and O 2p atomic orbitals. In

(16) (a) Greenwood, N. N.; Earnshaw, A. *Chemistry of the Elements*; Pergamon Press: Elmsford, NY, 1984; p 32. (b) Simon, A. *Angew. Chem., Int. Ed. Engl.* 1981, 20, 1013; 1988, 27, 160.

(17) Trietel, I. M.; Flood, M. T.; Marsh, R. E.; Gray, H. B. *J. Am. Chem. Soc.* 1969, 91, 6512.

(18) (a) Rocklage, S. M.; Turner, H. W.; Fellmann, J. D.; Schrock, R. R. *Organometallics* 1982, 1, 703. (b) Rocklage, S. M.; Schrock, R. R. *J. Am. Chem. Soc.* 1982, 104, 3077.

(19) Churchill, M. R.; Wasserman, H. J. *Inorg. Chem.* 1982, 21, 218.

(20) O'Regan, M. B.; Liu, A. H.; Finch, W. C.; Schrock, R. R.; Davis, W. M. *J. Am. Chem. Soc.* 1990, 112, 4331.

(21) Schrock, R. R.; Kolodziej, R. M.; Liu, A. H.; Davis, W. M.; Vale, M. G. *J. Am. Chem. Soc.* 1990, 112, 4338.

(22) Manriquez, J. M.; Sanner, R. D.; Marsh, R. E.; Bercaw, J. E. *J. Am. Chem. Soc.* 1976, 98, 3042.

(23) Chisholm, M. H.; Folting, K.; Huffman, J. C.; Kirkpatrick, C. C. *Inorg. Chem.* 1984, 23, 1021.

(24) Hall, M. B.; Fenske, R. F. *Inorg. Chem.* 1972, 11, 768.

(25) Bursten, B. E.; Jensen, J. R.; Fenske, R. F. *J. Chem. Phys.* 1978, 68, 3320.

the basis function for tungsten, the exponents for the 6s and 6p orbitals were both fixed at 1.80. All calculations were converged with a self-consistent-field iterative technique using a convergence criteria of 0.0010 as the largest deviation of atomic orbital populations between successive cycles.

Acknowledgment. We thank the National Science Foundation for financial support. R.H.C. is a National

Science Foundation Postdoctoral Fellow.

Registry No. 1, 137122-24-8.

Supplementary Material Available: Listings of anisotropic thermal parameters and all bond distances and angles and VER-SORT drawings (8 pages); a listing of F_o and F_c (6 pages). Ordering information is given on any current masthead page.

Organometallic Oxides: Preparation and Properties of the Diamagnetic Trinuclear Cluster $\{[(\eta\text{-C}_5\text{Me}_5)\text{Nb}(\mu\text{-Cl})(\mu\text{-O})]_3\}^+$ and Related Chloride-Oxides of Niobium

Frank Bottomley* and Selami Karslioglu†

Department of Chemistry, University of New Brunswick, Fredericton, New Brunswick, Canada E3B 5A3

Received July 1, 1991

Oxidation of $(\eta\text{-C}_5\text{Me}_5)_2\text{NbCl}_2$ with O_2 in tetrahydrofuran containing traces of water gave $[(\eta\text{-C}_5\text{Me}_5)\text{NbCl}_2]_2(\mu\text{-Cl})(\mu\text{-OH})(\mu\text{-O})$ (1) and polymeric $[\text{Nb}_2\text{Cl}_2\text{O}_4(\text{thf})_3]_n$. Complex 1 (for which a newly refined structure is reported) existed as two isomers, which are distinguished by the relative orientation of $\eta\text{-C}_5\text{Me}_5$ and the bridging ligands. Reduction of 1 with zinc powder gave $\{[(\eta\text{-C}_5\text{Me}_5)\text{Nb}(\mu\text{-Cl})(\mu\text{-O})]_3\}^+$ (2^+), which was isolated in combination with three different anions: $\{[\text{ZnCl}_2(\mu\text{-Cl})]_2\}^{2-}$, $\{[\text{ZnCl}]_4(\mu\text{-Cl})_6\}^{2-}$, and $\{[\text{ZnCl}]_6(\mu\text{-Cl})_8\}^{2-}$. Cluster 2^+ contained Nb_3^{13+} , was diamagnetic, and had an equilateral triangle of Nb atoms (average Nb-Nb distance 2.876 (1) Å), each edge of which was bridged by Cl and O atoms (average Nb-Cl = 2.542 (1) Å, average Nb-O 1.937 (3) Å). The geometry and electronic structure of 2^+ are compared with those of $\{[(\eta\text{-C}_5\text{Me}_5)\text{Re}(\mu\text{-O})_2]_3\}^{2+}$ and $\{[(\eta\text{-C}_6\text{Me}_6)\text{Nb}(\mu\text{-Cl})_2]_3\}^{n+}$ ($n = 1, 2$). The structure of the $\text{Zn}_4\text{Cl}_{10}^{2-}$ salt of 2^+ was reported previously. The $\text{Zn}_2\text{Cl}_6^{2-}$ salt was monoclinic, space group $A2/m$, $a = 14.7497$ (8) Å, $b = 16.311$ (2) Å, $c = 16.410$ (2) Å, $\beta = 95.67$ (1)°, $Z = 2$ (of $\{2\}[\text{Zn}_2\text{Cl}_6\text{C}_6\text{H}_{14}]$), and $R = 0.040$. The $\text{Zn}_6\text{Cl}_{14}^{2-}$ salt was triclinic, $P\bar{1}$, $a = 11.141$ (4) Å, $b = 14.793$ (7) Å, $c = 14.792$ (5) Å, $\alpha = 74.14$ (4)°, $\beta = 77.40$ (3)°, $\gamma = 77.32$ (4)°, $Z = 2$ (of $\{2\}[\text{Zn}_3\text{Cl}_7]$), and $R = 0.104$. Oxidation of the salts of 2^+ in CH_2Cl_2 solution with O_2 gave $\{[(\eta\text{-C}_5\text{Me}_5)\text{NbCl}]_3(\mu\text{-Cl})(\mu\text{-O})_2(\mu_3\text{-OH})(\mu_3\text{-O})\}^+$ (3^+), isolated as the $\{[\text{ZnCl}_2(\mu\text{-Cl})]_2\}^{2-}$ salt. Cluster 3^+ had an isosceles triangle of Nb atoms (Nb-Nb = 3.028 (2) Å ($\times 2$) and 3.318 (2) Å). The long Nb-Nb edge was bridged by Cl. The $\mu_3\text{-O}$ ligand had much shorter distances to the two Nb atoms forming the long edge (average 2.046 (8) Å) than to the third Nb (2.228 (8) Å). The $\mu_3\text{-OH}$ ligand had equal distances to all three Nb atoms (average 2.207 (8) Å). The salt $\{3\}[\text{Zn}_2\text{Cl}_6]$ was monoclinic, $P2_1/a$, $a = 11.377$ (1) Å, $b = 30.630$ (2) Å, $c = 11.442$ (1) Å, $\beta = 100.82$ (1)°, $Z = 4$ (of $\{3\}[\text{ZnCl}_3]$), and $R = 0.070$. The physical and chemical properties of 2^+ and 3^+ are reported and compared to those of related compounds.

Introduction

We have been synthesizing (cyclopentadienyl)metal oxides by two methods: oxidative aggregation of low-valent (cyclopentadienyl)metal derivatives (for example the preparation of $[(\eta\text{-C}_5\text{Me}_5)\text{Cr}(\mu_3\text{-O})]_4$ by oxidation of $(\eta\text{-C}_5\text{Me}_5)_2\text{Cr}$ with N_2O^1); reductive aggregation of high-valent (cyclopentadienyl)metal oxo complexes (for example the preparation of $\{[(\eta\text{-C}_5\text{H}_5)\text{MoCl}]_4(\mu\text{-O})_6\}[\text{ZnCl}(\text{thf})_2]$ by reduction of $(\eta\text{-C}_5\text{H}_5)\text{MoCl}_2(\text{O})$ with zinc powder²). We have also reported recently the preparation of the trinuclear oxide $[(\eta\text{-C}_5\text{H}_5)\text{NbCl}(\mu\text{-Cl})]_3(\mu_3\text{-OH})(\mu_3\text{-O})^3$ by the reduction of $[(\eta\text{-C}_5\text{H}_5)\text{NbCl}_3(\text{H}_2\text{O})_2(\mu\text{-O})]^{4-7}$ with aluminum powder.⁸ Attempts to reduce $[(\eta\text{-C}_5\text{H}_5)\text{NbCl}(\mu\text{-Cl})]_3(\mu_3\text{-OH})(\mu_3\text{-O})$ further (our goal being $[(\eta\text{-C}_5\text{H}_5)\text{Nb}]_5(\mu_3\text{-O})_6$, which would be the niobium analogue of $[(\eta\text{-C}_5\text{H}_5)\text{V}]_5(\mu_3\text{-O})_6$ ⁹) gave only intractable products. Therefore, we have turned to the $\eta\text{-C}_5\text{Me}_5$ derivatives of niobium. As with the $\eta\text{-C}_5\text{H}_5$ complexes, suitable starting materials for either oxidative or reductive aggregation are not readily available. Of the obvious choices for oxidative aggregation,

neither $(\eta\text{-C}_5\text{Me}_5)_2\text{Nb}$ nor $(\eta\text{-C}_5\text{Me}_5)\text{Nb}(\text{CO})_4$ is known, although the tantalum analogue of the latter has been prepared.^{10,11} The obvious choice for reductive aggregation is $(\eta\text{-C}_5\text{Me}_5)\text{NbCl}_2(\text{O})$, the vanadium analogue of which has been investigated extensively.¹²⁻¹⁶ However, this too is

(1) Bottomley, F.; Chen, J.; MacIntosh, S. M.; Thompson, R. C. *Organometallics* 1991, 10, 906.

(2) Bottomley, F.; Ferris, E. C.; White, P. S. *Organometallics* 1990, 9, 1166.

(3) Curtis, M. D.; Real, J. *Inorg. Chem.* 1988, 27, 3176.

(4) Daran, J.-C.; Prout, K.; De Cian, A.; Green, M. L. H.; Sigantporia, N. J. *Organomet. Chem.* 1977, 136, C4.

(5) Prout, K.; Daran, J.-C. *Acta Crystallogr.* 1979, B35, 2882.

(6) Andreu, A. M.; Jalón, F. A.; Otero, A.; Royo, P.; Lanfredi, A. M. M.; Tiripicchio, A. *J. Chem. Soc., Dalton Trans.* 1987, 953.

(7) Jalón, F. A.; Otero, A.; Royo, P.; Fernandez-G., J. M.; Rosales, M. J.; Toscano, R. A. *J. Organomet. Chem.* 1987, 331, C1.

(8) Bottomley, F.; Keizer, P. N.; White, P. S.; Preston, K. F. *Organometallics* 1990, 9, 1916.

(9) Bottomley, F.; Paez, D. E.; White, P. S. *J. Am. Chem. Soc.* 1983, 104, 5651.

(10) Gibson, V. C.; Kee, T. P.; Clegg, W. *J. Chem. Soc., Dalton Trans.* 1990, 3199.

(11) Herrmann, W. A.; Kalcher, W.; Biersack, H.; Bernal, I.; Creswick, M. *Chem. Ber.* 1981, 114, 3558.

(12) Bottomley, F.; Darkwa, J.; Sutin, L. C.; White, P. S. *Organometallics* 1986, 5, 2165.

(13) Bottomley, F.; Sutin, L. C. *J. Chem. Soc., Chem. Commun.* 1987, 1112.

* To whom correspondence should be addressed.

† Permanent address: Department of Chemistry, Karadeniz Technical University, Trabzon, Turkey.